

Displaced Photon Signal from a Light Scalar in Minimal Left-Right Symmetric Model

P. S. Bhupal Dev^a, Rabindra N. Mohapatra^b, Yongchao Zhang^c

^a*Department of Physics and McDonnell Center for the Space Sciences, Washington University, St. Louis, MO 63130, USA*

^b*Maryland Center for Fundamental Physics, Department of Physics,
University of Maryland, College Park, MD 20742, USA*

^c*Service de Physique Théorique, Université Libre de Bruxelles,
Boulevard du Triomphe, CP225, 1050 Brussels, Belgium*

We point out that in the minimal left-right realization of TeV scale seesaw for neutrino masses, the neutral scalar from the right-handed $SU(2)_R$ breaking sector could be much lighter than the right-handed scale. We discuss for the first time the constraints on this particle from low-energy flavor observables, find that the light scalar is necessarily long-lived. We show that it can be searched for at the LHC via displaced signals of a collimated photon jet, and can also be tested in current and future high-intensity experiments. In contrast to the unique diphoton signal (and associated jets) in the left-right case, a generic beyond Standard Model light scalar decays mostly to leptons or jets. Thus, the diphoton channel proposed here provides a new avenue to test the left-right framework and reveal the underlying neutrino mass generation mechanism.

I. INTRODUCTION

The discovery of neutrino masses has provided the first laboratory evidence for physics beyond the Standard Model (SM). The nature of the underlying new physics is however unclear and an “all hands on deck” approach is called for to pinpoint this, since the result would have a profound impact on the ongoing new physics searches by narrowing the beyond SM landscape. We explore this question using the seesaw paradigm [1] which is a simple and well motivated way to understand neutrino masses, and considering its ultraviolet-complete realization within a TeV-scale left-right symmetric model (LRSM) framework [2], based on the gauge group $\mathcal{G}_{LR} \equiv SU(2)_L \times SU(2)_R \times U(1)_{B-L}$.

The experimental signals of this model have been extensively studied in the literature, and generally involve the heavy gauge bosons and heavy right-handed neutrinos (RHNS) [3–5] or heavy Higgs bosons [6–9]. Here we propose a new complementary probe involving the LR symmetry breaking scalar sector, which is intimately related to the neutrino mass generation.

For the first time, we point out that the $SU(2)_R$ breaking scalar (denoted here by H_3) could be much lighter than the right-handed scale v_R . Unlike the heavy- H_3 case, a light H_3 could be produced (off-shell) in e.g. K and B mesons, through its mixing with other scalars, and therefore its couplings are tightly constrained by the low-energy flavor changing neutral current (FCNC) data. In consequence, it decays mostly into two photons via the $SU(2)_R$ gauge interaction, which is suppressed by the right-handed scale v_R . This naturally pushes H_3 to be a long-lived particle, with the (Lorentz-boosted) decay length clearly dictated by v_R and its mass. This is likely to be seen in high-intensity experiments, like SHiP and DUNE, and the high-energy collider LHC, in the latter it appears as a displaced vertex. The (displaced) photon signal could provide important information on the right-handed scale v_R and the seesaw mechanism, in a way that is largely complementary to other probes of the LRSM. This is

a specific feature of the LRSM that distinguishes it from other beyond SM light Higgs scenarios; for example in general models, a light scalar could mix with the SM Higgs and decay mostly into hadron jets and/or leptons. The (displaced) diphoton signal from light scalar decay could therefore be viewed, in some sense, as a “smoking-gun” signal of the LRSM.

II. LIGHT NEUTRAL SCALAR

The minimal LRSM consists of the following Higgs fields:

$$\Phi = \begin{pmatrix} \phi_1^0 & \phi_2^+ \\ \phi_1^- & \phi_2^0 \end{pmatrix}, \quad \Delta_R = \begin{pmatrix} \Delta_R^+/\sqrt{2} & \Delta_R^{++} \\ \Delta_R^0 & -\Delta_R^+/\sqrt{2} \end{pmatrix}, \quad (1)$$

which transform under \mathcal{G}_{LR} as $(2, 2, 0)$ and $(1, 3, 2)$, respectively. The group \mathcal{G}_{LR} is broken down to the EW gauge group by the triplet vacuum expectation value (VEV) $\langle \Delta_R^0 \rangle = v_R$, whereas the EW symmetry is broken by the bidoublet VEV $\langle \Phi \rangle = \text{diag}(\kappa, \kappa')$, with the EW VEV $v_{EW} = \sqrt{\kappa^2 + \kappa'^2}$. For simplicity, we assume that the discrete parity symmetry has been broken at a scale much larger than the $SU(2)_R$ -breaking scale [10], but our conclusions remain unchanged in the TeV-scale fully parity-symmetric version of the LRSM.

The most general scalar potential involving Φ and Δ_R is given in Eq. (A.1) in the appendix. One physical scalar from the bidoublet is identified as the SM Higgs h , while the other 4 degrees from the heavy doublet (H_1, A_1, H_1^\pm) have nearly degenerate mass, which is constrained to be $\gtrsim 10$ TeV from FCNC constraints [11]. Similarly, the mass of the doubly-charged scalars $H_2^{\pm\pm}$ from Δ_R is required to be above a few hundred GeV from same-sign dilepton pair searches at the LHC [9]. However, no constraint is available in the literature for the remaining neutral scalar field H_3 , consisting predominantly of the real component of Δ_R^0 . This is mainly due to the fact that it has no direct couplings to the SM sector and couples only to the heavy $SU(2)_R$ particles, in the limit of no mixing with other scalars. Therefore, its tree-level mass could in principle be much lower than the v_R scale, as long as the quartic coupling $\rho_1 \ll 1$ [cf. Eq. (A.4)]. This makes

it the only possible light scalar in the model, and due to its suppressed couplings to the SM sector, it is also a natural LLP candidate at the LHC and in future colliders.

Since we envision that H_3 mass is much less than the v_R scale, it is important to consider the loop corrections and see whether this small mass is radiatively stable. Recall that in the SM, if we neglect the one-loop fermion contributions to the Coleman-Weinberg effective potential [12], there is a lower limit of order of 5 GeV on the Higgs boson mass [13]. This bound goes away once the top-quark Yukawa coupling is included. Similarly, it was pointed out in Ref. [14] that in a class of LRSM, there is a lower bound of about 900 GeV on the real part of the doublet scalar field coming from purely gauge contributions. Inclusion of the Yukawa interactions to the RHNs in the minimal LRSM we are considering allows us to avoid this bound and have a very light H_3 .

Quantitatively, keeping only the Δ_R^0 terms in the one-loop effective potential [15], we obtain the correction term

$$\frac{3}{2\pi^2} \left[\frac{1}{3}\alpha_3^2 + \frac{8}{3}\rho_2^2 - 8f^4 + \frac{1}{2}g_R^4 + (g_R^2 + g_{BL}^2)^2 \right] v_R^2, \quad (2)$$

where g_R and g_{BL} are respectively the $SU(2)_R$ and $U(1)_{B-L}$ gauge coupling strengths. We have assumed the three RHNs in the LRSM to be approximately degenerate with the same Yukawa coupling f . From Eq. (2), one would naively expect the loop correction to be of order $v_R/4\pi$. However, the bosonic and fermionic contributions can cancel each other; with a mild tuning of g_R and f at the level of $\text{GeV}/v_{\text{EW}} \simeq 10^{-2}$, we can easily obtain a loop correction at or below the GeV scale. It is remarkable to note that the TeV scale seesaw prefers the natural value for Majorana Yukawa couplings to be of order one, implying in turn TeV scale RHNs with observable same-sign dilepton plus dijet signatures at the LHC [3].

III. COUPLINGS AND DECAY

When the mass of H_3 is well below the EW scale, which is our focus in this letter, it decays to the light SM fermions through mixing with the SM Higgs h and the heavy CP -even scalar H_1 from Φ , with the mixing angles respectively given by

$$\sin \theta_1 \simeq \frac{\alpha_1}{2\lambda_1} \frac{v_R}{v_{\text{EW}}}, \quad \sin \theta_2 \simeq \frac{4\alpha_2}{\alpha_3} \frac{v_{\text{EW}}}{v_R}. \quad (3)$$

Note the *inverted* dependence on the VEV ratio $(v_{\text{EW}}/v_R)^{-1}$ for the $h - H_3$ mixing, because the SM Higgs boson mass is of order of v_{EW} . The quartic couplings $\alpha_{1,2}$ connect H_3 to h and H_1 respectively. There is an alignment limit of the parameter space for $\alpha_{1,2} \rightarrow 0$, when H_3 is secluded from mixing with other scalars in the LRSM, and λ_1 approaches to $\lambda_{\text{SM}} = m_h^2/4v_{\text{EW}}^2$. Thus for TeV-scale v_R , both the mixing angles $\sin \theta_{1,2}$ are *naturally* small.

At the one-loop level, the gauge and Yukawa couplings induce the decay of H_3 into digluons and diphotons, as in the SM Higgs case. However, when the FCNC constraints on the mixing angles $\sin \theta_{1,2}$ are considered (see below), the dipho-

ton channel is dominated by the W_R loop which is suppressed only by the RH scale v_R : $\Gamma_{\gamma\gamma} \propto v_R^{-2}$ but not sensitive to the gauge coupling g_R . The heavy charged scalar loops (H_1^\pm and $H_2^{\pm\pm}$) are subleading, suppressed by a factor of $-5/21$ [cf. Eq. (A.10)]. The SM W loop is heavily suppressed by the $W - W_R$ mixing. All the couplings and partial decay widths of H_3 are collected in the appendix.

Contours of fixed decay length L_0 of H_3 at rest are shown in the $m_{H_3} - \sin \theta_1$ plane of Fig. 1 (dashed grey lines). For concreteness, we have made the following reasonable assumptions: (i) The RH scale $v_R = 5$ TeV, which is the smallest value required to satisfy the current LHC limits on W_R mass. We also set the $H_3 - H_1$ mixing $\sin \theta_2 = 0$. (ii) In the minimal LRSM, the RH quark mixing V_R is very similar to the CKM matrix V_L , up to some additional phases [16]. For simplicity we adopt $V_R = V_L$ in the calculation. (iii) The couplings to charged leptons depend on the heavy and light neutrino sector via the Yukawa coupling matrix $Y_{\nu N}$. Here we assume the light neutrinos are of normal hierarchy with the lightest neutrino mass of 0.01 eV and the three RHNs degenerate at 1 TeV without any RH lepton mixing, which pushes the couplings $Y_{\nu N} \sim 10^{-7}$. Furthermore, the flavor-changing decay modes are included, such as $H_3 \rightarrow sb, \mu\tau$, and the running of strong coupling α_s is taken into consideration, which is important below the EW scale.

From the lifetime curves in Fig. 1, it is clear that when m_{H_3} is below a few GeV, it tends to be long-lived, with decay lengths $L \gtrsim 0.01b$ cm (where $b = E_{H_3}/m_{H_3}$ is the Lorentz boost factor, whose distribution typically peaks at around 100 for a GeV-scale H_3 produced at the LHC energy), as long as the mixing angles $\sin \theta_{1,2}$ are small $\lesssim 10^{-4}$, which is guaranteed by the flavor constraints, as discussed below. With the couplings to fermions constrained by the flavor data, only the diphoton channel is significant, implying that H_3 decays mostly into two *displaced* photons at the LHC.

We should mention here that, on the cosmological side, when H_3 mass is below ~ 50 MeV, it will start contributing to dark radiation as $\Delta N_{\text{eff}} \simeq 4/7$, which is ruled out by the Planck data [17] at the 2.5σ C.L. Therefore, we will consider only H_3 with mass $\gtrsim 50$ MeV in the following.

IV. LOW-ENERGY FLAVOR CONSTRAINTS

Due to its mixing with the SM Higgs h and the heavy scalar H_1 , the light scalar H_3 induces flavor-changing couplings to the SM quarks, which are severely constrained by the low-energy flavor data, e.g. from $K - \bar{K}$, $B_d - \bar{B}_d$ and $B_s - \bar{B}_s$ neutral meson mixing, as well as rare K and B meson decays to lighter mesons and a photon pair. Although the couplings originate from the FCNC couplings of H_1 , as the masses of H_1 and H_3 are independent observables, the flavor constraints on H_3 derived below are different from those on the heavy scalar H_1 [11].

Taking the $K^0 - \bar{K}^0$ mixing as an explicit example, we cast the flavor-changing four-fermion interactions mediated by H_3 into a linear combination of the effective dimension-6 operators of the form

$$\mathcal{O} = \mu_{RL}^2 \mathcal{O}_2 + \mu_{LR}^2 \tilde{\mathcal{O}}_2 + 2\mu_{RL}\mu_{LR} \mathcal{O}_4, \quad (4)$$

where $\mu_{RL,LR} = \sum_i m_i \lambda_i^{RL,LR}$ with $m_i = \{m_u, m_c, m_t\}$ the running up-type quark masses, $\lambda_i^{LR} = V_{L,i2}^* V_{R,i1}$ and $\lambda_i^{RL} = V_{R,i2}^* V_{L,i1}$ the left- and right-handed quark mixing matrix elements, and $\mathcal{O}_2 = (\bar{s}P_L d)(\bar{s}P_L d)$, $\tilde{\mathcal{O}}_2 = (\bar{s}P_R d)(\bar{s}P_R d)$, $\mathcal{O}_4 = (\bar{s}P_L d)(\bar{s}P_R d)$ with $P_{L,R} = \frac{1}{2}(1 \mp \gamma_5)$ [18]. The effective Lagrangian we need is thus given by

$$\mathcal{L}_{H_3}^K = \frac{G_F}{\sqrt{2}} \frac{\sin^2 \tilde{\theta}_2}{m_K^2 - m_{H_3}^2 + im_{H_3} \Gamma_{H_3}} \mathcal{O}, \quad (5)$$

where G_F is the Fermi constant and $\sin \tilde{\theta}_2 = \sin \theta_2 + \xi \sin \theta_1$ is the ‘‘effective’’ mixing angle, which also involves the mixing with the SM Higgs, as h mixes with H_1 with a small angle $\xi = \kappa'/\kappa \simeq m_b/m_t$ [7]. Although the flavor-changing couplings of H_3 arise from its mixing with H_1 , the effective Lagrangian (5) is not simply multiplied by a factor of $\sin \tilde{\theta}_2$; in particular, the operators of form \mathcal{O}_2 and $\tilde{\mathcal{O}}_2$ are absent in the H_1 case, which are canceled by the CP -odd scalar A_1 in the mass degenerate limit of $m_{H_1} = m_{A_1}$. In Eq. (4), the charm quark contribution $m_c \lambda$ dominates (λ being the Cabibbo angle), with a subleading contribution $\sim m_t \lambda^5$ from the top quark.

Given the Lagrangian Eq.(5), it is straightforward to calculate the contribution of H_3 to the $K^0 - \bar{K}^0$ mixing, we need the hadronic matrix elements when the operators \mathcal{O}_2 , $\tilde{\mathcal{O}}_2$ and \mathcal{O}_4 are sandwiched by the K^0 states,

$$\langle K^0 | \mathcal{O}_i | \bar{K}^0 \rangle = N_i m_K f_K^2 B_i(\mu) R_K^2(\mu), \quad (6)$$

with $i=2, 4$, and $N_2 = 5/3$, $N_4 = -2$, $B_2 = 0.679$, $B_4 = 0.810$ from lattice calculation [18] and the kaon decay constant $f_K = 113$ MeV. The mass ratio $R_K = m_K/(m_d + m_s)$ is evaluated at the energy scale $\mu = 2$ GeV. As the strong interaction conserves parity, we have $\langle K^0 | \tilde{\mathcal{O}}_2 | \bar{K}^0 \rangle = \langle K^0 | \mathcal{O}_2 | \bar{K}^0 \rangle$. Then the K^0 mass difference

$$\Delta m_K \simeq 2 \text{Re} \eta_i(\mu) \langle K^0 | \mathcal{L}_{H_3}^K | \bar{K}^0 \rangle, \quad (7)$$

with $\eta_2 = 2.052$ and $\eta_4 = 3.2$ the the NLO QCD factors at $\mu = 2$ GeV [19].

Requiring that the light H_3 -mediated contribution be consistent with the current data on Δm_K , i.e. $< 1.74 \times 10^{-12}$ MeV [20], leads to an upper limit on the mixing angles $\sin \theta_{1,2}$, as presented in Fig. 1 (solid red line) for θ_1 (the limit on θ_2 is stronger by a factor of $\xi^{-1} \simeq m_t/m_b$). As expected from the propagator structure in Eq. (5), the limits on the mixing angles $\sin \theta_{1,2}$ are significantly strengthened in the narrow resonance region where $m_{H_3} \simeq m_K$. For $m_{H_3} \ll m_K$, the H_3 propagator is dominated by the momentum term: $(q^2 - m_{H_3}^2 + im_{H_3} \Gamma_{H_3})^{-1} \simeq q^{-2} \simeq m_K^{-2}$, and the limit approaches to a constant value, whereas for $m_{H_3} \gg m_K$, the limit scales as m_{H_3} .

The calculation of flavor constraints from B_d and B_s mixing are quite similar to those from K^0 [21]. with the QCD correction coefficients $\eta_2 = 1.654$ and $\eta_4 = 2.254$ [19], and the B -parameters $B_2(B_d) = 0.82$, $B_4(B_d) = 1.16$, $B_2(B_s) = 0.83$ and $B_4(B_s) = 1.17$ [22]. Unlike the K^0 case, the top-quark contribution dominates the effective coupling $\sum_i m_i \lambda_i^{LR,RL}$ and strengthens the corresponding limits

on the couplings of H_3 to the bottom quark. The mixing limits from $\Delta m_{B_d} < 9.3 \times 10^{-11}$ MeV and $\Delta m_{B_s} < 2.7 \times 10^{-9}$ MeV are shown in Fig. 1, respectively, as the solid blue and cyan lines. The B mesons are 10 times heavier than the K meson, and the absolute values of error bars for Δm_B are much larger than that for Δm_K ; this makes the B -mixing limits weaker than K -mixing limit for $m_{H_3} \ll m_B$. However, this could be partially compensated by the large effective coupling $\sum_i m_i \lambda_i^{LR}$ when H_3 is heavier. Thus for $m_{H_3} \gtrsim 1$ GeV, the limits on $\sin \theta_{1,2}$ from the B_d -mixing turn out to be more stringent.

A light H_3 could also be produced in rare meson decays via the flavor-changing couplings, if kinematically allowed. The corresponding SM decay modes are either forbidden or highly suppressed by loop factors and the CKM matrix elements; thus these rare decay channels are also expected to set stringent limits on $\sin \theta_{1,2}$. We consider the decays $B \rightarrow KH_3$ and $K \rightarrow \pi H_3$ each followed by $H_3 \rightarrow \chi\chi$, with $\chi = e^+e^-$, $\mu^+\mu^-$, $\gamma\gamma$. The rare SM processes $K \rightarrow \pi\chi\chi$ and $B \rightarrow K\chi\chi$ has been searched for in NA48/2 [23, 24], NA62 [25], KTeV [26–29], BaBar [30], Belle [31], LHCb [32]. The limits on the mixing angle $\sin \theta_1$ are collectively depicted in Fig. 1, where conservatively we demand H_3 decays inside the detector spatial resolution $L_{H_3} < 0.1$ mm, and the branching ratios $\text{BR}(H_3 \rightarrow \chi\chi)$ and Lorentz boost factor E_{H_3}/m_{H_3} from meson decay have been taken into consideration. More details can be found in Ref. [21].

After being produced from meson decay, if H_3 decays outside the detector, the signal is $d_j \rightarrow d_i$ at the parton level plus missing energy. This could be constrained by the current limits of $K \rightarrow \pi\nu\bar{\nu}$ from E949 [33–36] and $B \rightarrow K\nu\bar{\nu}$ from BaBar [37], and future prospects at NA62 [38] and Belle II [39], which are all presented in Fig. 1. As light H_3 tends to be long-lived, the ‘‘invisible’’ searches with neutrinos in the final state are more constraining than ‘‘visible’’ decay modes above. With a huge number of protons-on-target and rather long decay length, the beam-dump experiments could further improve the limits. The current limits from CHARM [40] and future prospects at SHiP [41] and DUNE [42] are also shown in Fig. 1, which could exclude the mixing angle up to the level of 10^{-13} .

The full details of the limits of rare K and B decays on the couplings of H_3 are presented in Ref. [21]. Here we list only the most important information which leads to the limits and prospects in Fig.2. As H_3 can have tree-level flavor-changing couplings to the SM quarks, the decay $d_j \rightarrow d_i H_3$ in the down-type quark sector might exceed the observed total widths of K and B mesons, as long as the mixing angles $\sin \theta_{1,2}$ are sufficiently large. Thus in all the calculations below, we incorporate also the constraints of $\Gamma(K \rightarrow \pi H_3) > \Delta\Gamma_{\text{total}}(K)$ and $\Gamma(B \rightarrow KH_3) > \Delta\Gamma_{\text{total}}(B)$, where, taking into consideration of the theoretical and experimental uncertainties, we use 20% of the total widths to set the limits. All the relevant rare decays

$$d_j \rightarrow d_i H_3 \quad \text{with} \quad H_3 \rightarrow e^+e^-, \mu^+\mu^-, \quad (\text{or } H_3 \rightarrow \text{any}) \quad (8)$$

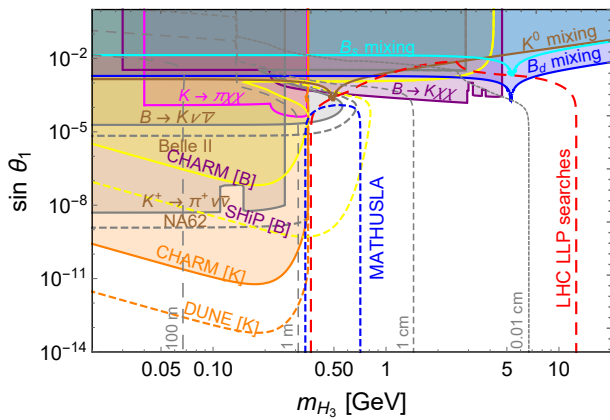


FIG. 1. Contours of H_3 decay length at rest (dashed gray lines) as functions of its mass and mixing with the SM Higgs boson. Superimposed are limits (color-shaded) from meson mixing (K^0 , $B_{d,s}$) and rare meson decays $K \rightarrow \pi\chi\chi$, $B \rightarrow K\chi\chi$ ($\chi = e, \mu, \gamma$), $K \rightarrow \pi\nu\bar{\nu}$, $B \rightarrow K\nu\bar{\nu}$ and $K \rightarrow \pi H_3 \rightarrow \pi\gamma\gamma$ and $B \rightarrow K H_3 \rightarrow K\gamma\gamma$ at beam-dump experiments. Also shown are the projected sensitivities from LLP searches at LHC and MATHUSLA.

are collected in Table I, where the readers can find also the expected *average* energies of H_3 from meson decay and the current and future limits. For the “visible” decays with leptons or photons in the final state, if the decay length of H_3 is significantly larger than the detector spatial resolutions, the displaced events could easily be identified in the high intensity experiments, thus we conservatively set the decay length to be $L_{H_3} < 0.1$ mm, where the Lorentz boost factor E_{H_3}/m_{H_3} has been taken into consideration. Regarding the B decays, when the H_3 mass is close to that of J/ψ or $\psi(2S)$, we use the SM branching ratios

$$\begin{aligned} \text{BR}(B \rightarrow K J/\psi) &= \text{BR}(B \rightarrow K \ell^+ \ell^-) = 5 \times 10^{-5}, \\ \text{BR}(B \rightarrow K \psi(2S)) &= \text{BR}(B \rightarrow K \ell^+ \ell^-) = 5 \times 10^{-6}. \end{aligned} \quad (9)$$

to set limits on H_3 . For the “invisible” decays with neutrinos in the final state, H_3 is required to be long-lived enough to decay outside the detectors. In the beam-dump experiments CHARM, SHiP and DUNE, the most stringent limits are from the diphoton modes $H_3 \rightarrow \gamma\gamma$, benefiting from the large branching ratio. Without any signal observed, CHARM sets an upper limit of $N_{\text{event}} < 2.3$ at the 90% C.L., while at the future experiments SHiP and DUNE, we assume the signal numbers to be less than 3. More calculation details can be found in Ref. [21].

Note that the mixing angle $\sin \theta_1$ could also be constrained by the precise Higgs measurements, invisible SM Higgs decay, rare decays $Z \rightarrow \gamma H_3$ and $t \rightarrow u H_3, c H_3$. However, these limits are much weaker than those from meson oscillation and decay, at most of order 0.1, and are not shown here.

V. DISPLACED DIPHOTON SIGNAL AT THE LHC

For a light H_3 with mass $\lesssim 10$ GeV, the $h - H_3$ mixing is so severely constrained that its Higgs portal production

is highly suppressed and it could only be produced via the gauge coupling through heavy vector boson fusion (VBF): $pp \rightarrow W_R^* W_R^* jj \rightarrow H_3 jj$, with a subleading contribution from Z_R fusion [7]. The associated production of $W_R H_3$ is further suppressed by the heavy gauge boson mass in the final state. When $m_{H_3} \lesssim 10$ GeV, the VBF production rate is almost constant for a given v_R , and is sensitive only to the gauge coupling g_R . For a smaller $g_R < g_L$, the W_R boson is lighter and the production of H_3 can be significantly enhanced.

Limited by the flavor data, a light H_3 decays mostly into the diphoton final state at the LHC after being produced. For a GeV mass, the decay-at-rest length L_0 is of order of cm; multiplied by a boost factor of $b \sim 100$, the actual decay length is expected to be of order of m, comparable to the radius of the Electromagnetic Calorimeter (ECAL) of ATLAS and CMS detectors, which are respectively 1.5 m [43] and 1.3 m [44]. The final-state photons from H_3 decay are highly collimated with a separation of $\Delta R \sim m_{H_3}/E_{H_3}$. Thus, most of the photon pairs can not be separated with the angular resolution of $\Delta\eta \times \Delta\phi = 0.025 \times 0.025$ (ATLAS) and 0.0174×0.0174 (CMS) [43, 44], and would be identified as a high-energy single-photon jet. Counting conservatively these single photon jets within $1 \text{ cm} < L < R_{\text{ECAL}}$, we can have up to thousands of signal events for an integrated luminosity of 3000 fb^{-1} at $\sqrt{s} = 14$ TeV LHC, depending on the RH scale v_R and gauge coupling g_R (see Fig. 2). The SM fake rate for the displaced diphotons is expected to be small [45], thus the displaced photon events, with the associated VBF jets, would constitute a new “smoking gun” signature of the H_3 decays as predicted by the minimal LRSM. For $m_{H_3} \lesssim 1$ GeV, the decay length exceeds the size of LHC detectors, but could be just suitable for future dedicated LLP search experiments, such as MATHUSLA [46], as shown in Fig. 1.

To have a better feeling of the displaced photon signal at the LHC and the dedicated long-lived particle surface detector MATHUSLA, we show here in Fig. 2 the expected numbers of signal events that could be collected in the ECAL of ATLAS and MATHUSLA, for the benchmark value of $v_R = 5$ TeV and $g_R/g_L = 0.6, 1$ and 1.5 . The basic trigger cuts $p_T > 25$ GeV and $\Delta\phi_{jj} > 0.4$ are applied to the VBF jets. As the diphotons from H_3 decay are highly boosted, with a factor of $E_{H_3}/m_{H_3} \sim 10^2$, the photon pairs are highly collimated, and, to be conservative, we consider only the events that can *not* be separated by the ATLAS detector. At ATLAS, the displaced photon-jet signal could reach up to thousands; while at the surface detector MATHUSLA the effective solid angle is much smaller, $\lesssim 0.1 \times 4\pi$, thus the events are much less. However, far away from the collision point, ultra displaced signal at MATHUSLA is expected to be almost background-free. The LLP searches at the general-purpose detector ATLAS/CMS and dedicated detector MATHUSLA are largely complementary to each other.

The projected probable regions in the plane of m_{H_3} and m_{W_R} are presented in Fig. 3, for three benchmark values of $g_R/g_L = 0.6, 1$ and 1.5 , where we have assumed 10 and 4 signal events of displaced photon jets at respectively LHC and MATHUSLA. As a result of the large Lorentz boost factors, the LLP searches at LHC and MATHUSLA are sensitive

TABLE I. Summary of meson decay constraints used to derive current/future limits in Fig.1. The last column gives the upper limit on the BR of the process used in our calculation. The corresponding numbers (in parenthesis) for the beam-dump experiments (last six rows) give the limit on the number of events. More details can be found in Ref. [21].

Experiment	Meson decay	H_3 decay	E_{H_3}	Decay length	Limit on BR (N_{event})
NA48/2	$K^+ \rightarrow \pi^+ H_3$	$H_3 \rightarrow e^+ e^-$	~ 30 GeV	< 0.1 mm	2.63×10^{-7}
NA48/2	$K^+ \rightarrow \pi^+ H_3$	$H_3 \rightarrow \mu^+ \mu^-$	~ 30 GeV	< 0.1 mm	8.88×10^{-8}
NA62	$K^+ \rightarrow \pi^+ H_3$	$H_3 \rightarrow \gamma\gamma$	~ 37 GeV	< 0.1 mm	4.70×10^{-7}
E949	$K^+ \rightarrow \pi^+ H_3$	any (inv.)	~ 355 MeV	> 4 m	4×10^{-10}
NA62	$K^+ \rightarrow \pi^+ H_3$	any (inv.)	~ 37.5 GeV	> 2 m	2.4×10^{-11}
KTeV	$K_L \rightarrow \pi^0 H_3$	$H_3 \rightarrow e^+ e^-$	~ 30 GeV	< 0.1 mm	2.8×10^{-10}
KTeV	$K_L \rightarrow \pi^0 H_3$	$H_3 \rightarrow \mu^+ \mu^-$	~ 30 GeV	< 0.1 mm	4×10^{-10}
KTeV	$K_L \rightarrow \pi^0 H_3$	$H_3 \rightarrow \gamma\gamma$	~ 40 GeV	< 0.1 mm	3.71×10^{-7}
BaBar	$B \rightarrow K H_3$	$H_3 \rightarrow \ell^+ \ell^-$	$\sim m_B/2$	< 0.1 mm	7.91×10^{-7}
Belle	$B \rightarrow K H_3$	$H_3 \rightarrow \ell^+ \ell^-$	$\sim m_B/2$	< 0.1 mm	4.87×10^{-7}
LHCb	$B^+ \rightarrow K^+ H_3$	$H_3 \rightarrow \mu^+ \mu^-$	~ 150 GeV	< 0.1 mm	4.61×10^{-7}
BaBar	$B \rightarrow K H_3$	any (inv.)	$\sim m_B/2$	> 3.5 m	3.2×10^{-5}
Belle II	$B \rightarrow K H_3$	any (inv.)	$\sim m_B/2$	> 3 m	4.1×10^{-6}
CHARM	$K \rightarrow \pi H_3$	$H_3 \rightarrow \gamma\gamma$	~ 10 GeV	[480, 515] m (< 2.3)	
CHARM	$B \rightarrow X_s H_3$	$H_3 \rightarrow \gamma\gamma$	~ 10 GeV	[480, 515] m (< 2.3)	
SHiP	$B \rightarrow X_s H_3$	$H_3 \rightarrow \gamma\gamma$	~ 25 GeV	[70, 125] m (< 3)	
DUNE	$K \rightarrow \pi H_3$	$H_3 \rightarrow \gamma\gamma$	~ 12 GeV	[500, 507] m (< 3)	

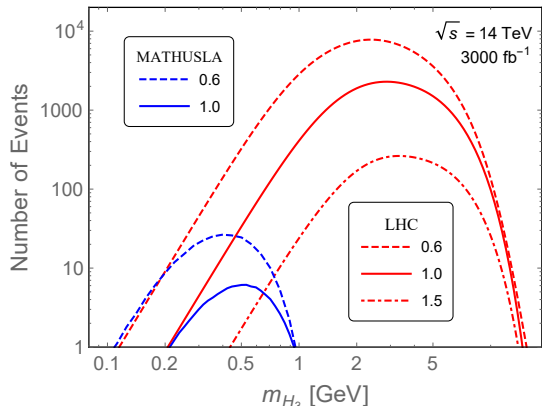


FIG. 2. Predicted numbers of displaced photon events from H_3 decay within the ECAL of ATLAS and the surface detector MATHUSLA, with an integrated luminosity of 3000 fb^{-1} at $\sqrt{s} = 14$ TeV, for $v_R = 5$ TeV and three benchmark values of $g_R/g_L = 0.6, 1$ and 1.5 .

to larger values of m_{H_3} , as compared to the low-energy meson decay searches, and are therefore complementary to the meson probes at the high intensity frontier, as clearly shown in Fig. 1. This is also largely complementary to the direct searches of W_R via same-sign dilepton plus jets in revealing the right-handed $SU(2)_R$ breaking and the TeV-scale seesaw mechanism at the high energy frontier, as shown in Fig. 3.

VI. SUMMARY

We have pointed out for the first time that, in the minimal

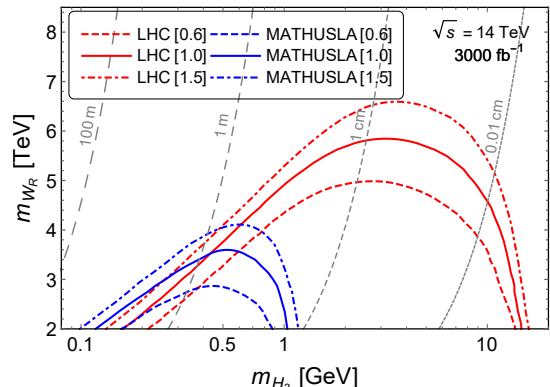


FIG. 3. Sensitivity contours in the $m_{H_3} - m_{W_R}$ plane from LLP searches at LHC and MATHUSLA, for $g_R/g_L = 0.6, 1$ and 1.5 . The grey contours indicate the proper lifetime of H_3 with $g_R = g_L$; for $g_R \neq g_L$, the lifetime has to be rescaled by the factor of $(g_R/g_L)^{-2}$.

LRSM the $SU(2)_R$ breaking scalar H_3 could be much lighter than the right-handed scale v_R , and searches for light H_3 via high energy displaced photon searches at the LHC provide a new probe of the TeV scale left-right seesaw models. We have derived the low energy flavor constraints on such particles, and given the predictions for the displaced photon signal from its production and decay at the LHC, as well as the prospects at the high-intensity frontier like SHiP and DUNE. Moreover, the dominant diphoton decay channel of the light scalar considered here is a unique feature of the LRSM that can be used to distinguish it from other beyond SM scenarios.

ACKNOWLEDGEMENT

The work of R.N.M. is supported by the US National Science Foundation grant No. PHY1620074. Y.Z. would like to

thank the IISN and Belgian Science Policy (IAP VII/37) for support.

Appendix: Scalar potential, couplings and decay widths of H_3

The most general renormalizable scalar potential for the Φ and Δ_R fields invariant under the gauge group \mathcal{G}_{LR} is given by

$$\begin{aligned} \mathcal{V} = & -\mu_1^2 \text{Tr}(\Phi^\dagger \Phi) - \mu_2^2 \left[\text{Tr}(\tilde{\Phi} \Phi^\dagger) + \text{Tr}(\tilde{\Phi}^\dagger \Phi) \right] - \mu_3^2 \text{Tr}(\Delta_R \Delta_R^\dagger) + \lambda_1 \left[\text{Tr}(\Phi^\dagger \Phi) \right]^2 + \lambda_2 \left\{ \left[\text{Tr}(\tilde{\Phi} \Phi^\dagger) \right]^2 + \left[\text{Tr}(\tilde{\Phi}^\dagger \Phi) \right]^2 \right\} \\ & + \lambda_3 \text{Tr}(\tilde{\Phi} \Phi^\dagger) \text{Tr}(\tilde{\Phi}^\dagger \Phi) + \lambda_4 \text{Tr}(\Phi^\dagger \Phi) \left[\text{Tr}(\tilde{\Phi} \Phi^\dagger) + \text{Tr}(\tilde{\Phi}^\dagger \Phi) \right] + \rho_1 \left[\text{Tr}(\Delta_R \Delta_R^\dagger) \right]^2 + \rho_2 \text{Tr}(\Delta_R \Delta_R) \text{Tr}(\Delta_R^\dagger \Delta_R^\dagger) \\ & + \alpha_1 \text{Tr}(\Phi^\dagger \Phi) \text{Tr}(\Delta_R \Delta_R^\dagger) + \left[\alpha_2 e^{i\delta_2} \text{Tr}(\tilde{\Phi}^\dagger \Phi) \text{Tr}(\Delta_R \Delta_R^\dagger) + \text{H.c.} \right] + \alpha_3 \text{Tr}(\Phi^\dagger \Phi \Delta_R \Delta_R^\dagger). \end{aligned} \quad (\text{A.1})$$

After symmetry breaking and diagonalization of the mass matrices, the physical scalar masses are given by

$$m_h^2 \simeq \left(4\lambda_1 - \frac{\alpha_1^2}{\lambda_1 - \rho_1} \right) \kappa^2, \quad (\text{A.2})$$

$$m_{H_1}^2 \simeq \alpha_3 (1 + 2\xi^2) v_R^2 + 4 \left(2\lambda_2 + \lambda_3 + \frac{4\alpha_2^2}{\alpha_3} \right) \kappa^2, \quad (\text{A.3})$$

$$m_{H_3}^2 \simeq 4\rho_1 v_R^2 + \left(\frac{\alpha_1^2}{\lambda_1 - \rho_1} - \frac{16\alpha_2^2}{\alpha_3} \right) \kappa^2, \quad (\text{A.4})$$

$$m_{A_1}^2 \simeq \alpha_3 (1 + 2\xi^2) v_R^2 + 4(\lambda_3 - 2\lambda_2) \kappa^2, \quad (\text{A.5})$$

$$m_{H_1^\pm}^2 \simeq \alpha_3 \left[(1 + 2\xi^2) v_R^2 + \frac{1}{2} \kappa^2 \right], \quad (\text{A.6})$$

$$m_{H_2^{\pm\pm}}^2 \simeq 4\rho_2 v_R^2 + \alpha_3 \kappa^2, \quad (\text{A.7})$$

where $\xi \equiv \kappa'/\kappa$ is the ratio of the bidoublet VEVs.

All the couplings of H_3 to the SM and heavy particles in the LRSM are given in Table II, which is based on the calculation of Ref. [7] and up to the leading order in the small parameters $\xi, \epsilon \equiv v_{EW}/v_R, \sin \tilde{\theta}_1 = \sin \theta_1 + \xi \sin \theta_2, \sin \tilde{\theta}_2 = \sin \theta_2 + \xi \sin \theta_1$. Here ϕ is defined as $\tan \phi \equiv g_{BL}/g_R$.

TABLE II. The couplings of a light scalar H_3 . The mixing angles θ_1 and θ_2 are defined in Eq. (3).

couplings	values	couplings	values
$H_3 h h$	$\frac{1}{\sqrt{2}} \alpha_1 v_R$	$H_3 W^+ W^-$	$\frac{1}{\sqrt{2}} g_L^2 \sin \theta_1 v_{EW} + \sqrt{2} g_R^2 \sin^2 \zeta_W v_R$
$h H_3 H_3$	$-\sqrt{2} \alpha_1 v_{EW}$	$H_3 W^+ W_R^-$	$\sqrt{2} g_R^2 \sin \zeta_W v_R$
$H_3 h H_1$	$2\sqrt{2} \alpha_2 v_R$	$H_3 W_R^+ W_R^-$	$\sqrt{2} g_R^2 v_R$
$H_3 H_1 H_1$	$\frac{1}{\sqrt{2}} \alpha_3 v_R$	$H_3 Z Z$	$\frac{g_L^2 \sin \theta_1 v_{EW}}{2\sqrt{2} \cos^2 \theta_W} + \frac{\sqrt{2} g_R^2 \sin^2 \zeta_Z v_R}{\cos^2 \phi}$
$H_3 A_1 A_1$	$\frac{1}{\sqrt{2}} \alpha_3 v_R$	$H_3 Z Z_R$	$-\frac{g_L g_R \sin \theta_1 \cos \phi v_{EW}}{\sqrt{2} \cos \theta_W} + \frac{2\sqrt{2} g_R^2 \sin \zeta_Z v_R}{\cos^2 \phi}$
$H_3 H_1^+ H_1^-$	$\sqrt{2} \alpha_3 v_R$	$H_3 Z_R Z_R$	$\frac{\sqrt{2} g_R^2 v_R}{\cos^2 \phi}$
$H_3 H_2^{++} H_2^{--}$	$2\sqrt{2} (\rho_1 + 2\rho_2) v_R$	$H_3 H_1^+ W^-$	$\frac{1}{2} g_L (\sin \theta_2 - \sin \theta_1 \xi)$
$H_3 \bar{u} u$	$\frac{1}{\sqrt{2}} \hat{Y}_U \sin \tilde{\theta}_1 - \frac{1}{\sqrt{2}} \left(V_L \hat{Y}_D V_R^\dagger \right) \sin \tilde{\theta}_2$	$H_3 H_1^+ W_R^-$	$\frac{1}{2} g_R \epsilon$
$H_3 \bar{d} d$	$\frac{1}{\sqrt{2}} \hat{Y}_D \sin \tilde{\theta}_1 - \frac{1}{\sqrt{2}} \left(V_L^\dagger \hat{Y}_U V_R \right) \sin \tilde{\theta}_2$	$H_3 A_1 Z$	$-\frac{i g_L (\sin \theta_2 - \sin \theta_1 \xi)}{2 \cos \theta_W}$
$H_3 \bar{e} e$	$\frac{1}{\sqrt{2}} \hat{Y}_E \sin \tilde{\theta}_1 - \frac{1}{\sqrt{2}} Y_{\nu N} \sin \tilde{\theta}_2$	$H_3 A_1 Z_R$	$\frac{i}{2} g_R (\sin \theta_2 - \sin \theta_1 \xi) \cos \phi$
$H_3 N N$	$\frac{M_N}{\sqrt{2} v_R}$		

The partial decay widths for the dominant decay modes of H_3 are collected below:

$$\Gamma(H_3 \rightarrow q\bar{q}) = \frac{3m_{H_3}}{16\pi} \left[\sum_{i,j} |\mathcal{Y}_{u,ij}|^2 \beta_2^3(m_{H_3}, m_{u_i}, m_{u_j}) \Theta(m_{H_3} - m_{u_i} - m_{u_j}) + \sum_{i,j} |\mathcal{Y}_{d,ij}|^2 \beta_2^3(m_{H_3}, m_{d_i}, m_{d_j}) \Theta(m_{H_3} - m_{d_i} - m_{d_j}) \right], \quad (\text{A.8})$$

$$\Gamma(H_3 \rightarrow \ell^+ \ell^-) = \frac{m_{H_3}}{16\pi} \sum_{i,j} |\mathcal{Y}_{e,ij}|^2 \beta_2^3(m_{H_3}, m_{e_i}, m_{e_j}) \Theta(m_{H_3} - m_{e_i} - m_{e_j}), \quad (\text{A.9})$$

$$\Gamma(H_3 \rightarrow \gamma\gamma) = \frac{\alpha^2 m_{H_3}^3}{1028\pi^3} \left| \frac{\sqrt{2}}{v_R} A_0(\tau_{H_1^\pm}) + \frac{4\sqrt{2}}{v_R} A_0(\tau_{H_2^{\pm\pm}}) + \frac{\sqrt{2}}{v_{EW}} \sum_{f=q,\ell} f_f N_C^f Q_f A_{1/2}(\tau_f) + \frac{\sqrt{2}}{v_R} A_1(\tau_{W_R}) \right|^2, \quad (\text{A.10})$$

$$\Gamma(H_3 \rightarrow gg) = \frac{G_F \alpha_s^2 m_{H_3}^3}{36\sqrt{2}\pi^3} \left| \frac{3}{4} \sum_{f=q} f_f A_{1/2}(\tau_f) \right|^2, \quad (\text{A.11})$$

with the kinetic function

$$\beta_2(M, m_1, m_2) \equiv \left[1 - \frac{2(m_1^2 + m_2^2)}{M^2} + \frac{(m_1^2 - m_2^2)^2}{M^4} \right]^{1/2}, \quad (\text{A.12})$$

the Yukawa couplings

$$\mathcal{Y}_u = \widehat{Y}_U \sin \tilde{\theta}_1 - (V_L \widehat{Y}_D V_R^\dagger) \sin \tilde{\theta}_2, \quad (\text{A.13})$$

$$\mathcal{Y}_d = \widehat{Y}_D \sin \tilde{\theta}_1 - (V_L^\dagger \widehat{Y}_U V_R) \sin \tilde{\theta}_2, \quad (\text{A.14})$$

$$\mathcal{Y}_e = \widehat{Y}_E \sin \tilde{\theta}_1 - Y_{\nu N} \sin \tilde{\theta}_2, \quad (\text{A.15})$$

f_f the normalization factor with respect to the SM Yukawa couplings,

$$f_{u,i} = \sin \tilde{\theta}_1 - \frac{(V_L \widehat{M}_d V_R^\dagger)_{ii}}{m_{u,i}} \sin \tilde{\theta}_2, \quad (\text{A.16})$$

$$f_{d,i} = \sin \tilde{\theta}_1 - \frac{(V_L^\dagger \widehat{M}_u V_R)_{ii}}{m_{d,i}} \sin \tilde{\theta}_2, \quad (\text{A.17})$$

$$f_{e,i} = \sin \tilde{\theta}_1 - \frac{Y_{\nu N,ii}}{m_{e,i}/v_{EW}} \sin \tilde{\theta}_2, \quad (\text{A.18})$$

and the loop functions

$$A_0(\tau) \equiv -[\tau - f(\tau)] \tau^{-2}, \quad (\text{A.19})$$

$$A_{1/2}(\tau) \equiv 2[\tau + (\tau - 1)f(\tau)] \tau^{-2}, \quad (\text{A.20})$$

$$A_1(\tau) \equiv -[2\tau^2 + 3\tau + 3(2\tau - 1)f(\tau)] \tau^{-2}, \quad (\text{A.21})$$

with $\tau_X = m_{H_3}^2/4m_X^2$ and

$$f(\tau) \equiv \begin{cases} \arcsin^2 \sqrt{\tau} & (\text{for } \tau \leq 1) \\ -\frac{1}{4} \left[\log \left(\frac{1+\sqrt{1-1/\tau}}{1-\sqrt{1-1/\tau}} \right) - i\pi \right]^2 & (\text{for } \tau > 1). \end{cases} \quad (\text{A.22})$$

For the heavy particle loops, only the large loop mass limit is useful for us: $A_0(0) = 1/3$, $A_{1/2}(0) = 4/3$, $A_1(0) = -7$. In this limit the gauge decay mode $\gamma\gamma$ is only sensitive to the RH scale v_R via $\Gamma \propto v_R^{-2}$. The contributions from the scalars H_1^\pm and $H_2^{\pm\pm}$ are suppressed by $5A_0(0)/A_1(0) = -5/21$, with the factor of 5 from sum of the electric charges squared.

- [1] P. Minkowski, Phys. Lett. B **67**, 421 (1977); R. N. Mohapatra and G. Senjanović, Phys. Rev. Lett. **44**, 912 (1980); T. Yanagida, Conf. Proc. C **7902131**, 95 (1979); M. Gell-Mann, P. Ramond and R. Slansky, Conf. Proc. C **790927**, 315 (1979) [[arXiv:1306.4669](#) [hep-th]]; S. L. Glashow, NATO Sci. Ser. B **61**, 687 (1980).
- [2] J. C. Pati and A. Salam, Phys. Rev. D **10**, 275 (1974); R. N. Mohapatra and J. C. Pati, Phys. Rev. D **11** 2558 (1975); G. Senjanović and R. N. Mohapatra, Phys. Rev. D **12** 1502 (1975).
- [3] W. Y. Keung and G. Senjanović, Phys. Rev. Lett. **50**, 1427 (1983); A. Ferrari *et al.*, Phys. Rev. D **62**, 013001 (2000); M. Nemevsek, F. Nesti, G. Senjanovic and Yue Zhang, Phys. Rev. D **83**, 115014 (2011) [[arXiv:1103.1627](#) [hep-ph]]; S. P. Das, F. F. Deppisch, O. Kittel and J. W. F. Valle, Phys. Rev. D **86**, 055006 (2012) [[arXiv:1206.0256](#) [hep-ph]]; J. A. Aguilar-Saavedra and F. R. Joaquim, Phys. Rev. D **86**, 073005 (2012) [[arXiv:1207.4193](#) [hep-ph]]; C. Y. Chen, P. S. B. Dev and R. N. Mohapatra, Phys. Rev. D **88**, 033014 (2013) [[arXiv:1306.2342](#) [hep-ph]]; J. Gluza and T. Jeliński, Phys. Lett. B **748**, 125 (2015) [[arXiv:1504.05568](#) [hep-ph]]; J. N. Ng, A. de la Puente and B. W. P. Pan, JHEP **1512**, 172 (2015) [[arXiv:1505.01934](#) [hep-ph]]; P. S. B. Dev, D. Kim and R. N. Mohapatra, JHEP **1601**, 118 (2016) [[arXiv:1510.04328](#) [hep-ph]]; M. Lindner, F. S. Queiroz, W. Rodejohann and C. E. Yaguna, JHEP **1606**, 140 (2016) [[arXiv:1604.08596](#) [hep-ph]]; M. Mitra, R. Ruiz, D. J. Scott and M. Spannowsky, Phys. Rev. D **94**, 095016 (2016) [[arXiv:1607.03504](#) [hep-ph]].
- [4] F. F. Deppisch, P. S. B. Dev and A. Pilaftsis, New J. Phys. **17**, 075019 (2015) [[arXiv:1502.06541](#) [hep-ph]].
- [5] V. Khachatryan *et al.* [CMS Collaboration], Eur. Phys. J. C **74**, 3149 (2014) [[arXiv:1407.3683](#) [hep-ex]]; G. Aad *et al.* [ATLAS Collaboration], JHEP **1507**, 162 (2015) [[arXiv:1506.06020](#) [hep-ex]]; V. Khachatryan *et al.* [CMS Collaboration], [arXiv:1612.01190](#) [hep-ex].
- [6] J. F. Gunion *et al.*, PRINT-86-1324 (UC,DAVIS); G. Azuelos, K. Benslama and J. Ferland, J. Phys. G **32**, 73 (2006) [[hep-ph/0503096](#)]; D. W. Jung and K. Y. Lee, Phys. Rev. D **78**, 015022 (2008) [[arXiv:0802.1572](#) [hep-ph]]; G. Bambhaniya, J. Chakraborty, J. Gluza, M. Kordiaczyska and R. Szafron, JHEP **1405**, 033 (2014) [[arXiv:1311.4144](#) [hep-ph]]; B. Dutta, R. Eusebi, Y. Gao, T. Ghosh and T. Kamon, Phys. Rev. D **90**, 055015 (2014) [[arXiv:1404.0685](#) [hep-ph]]; G. Bambhaniya, J. Chakraborty, J. Gluza, T. Jelinski and R. Szafron, Phys. Rev. D **92**, 015016 (2015) [[arXiv:1504.03999](#) [hep-ph]].
- [7] P. S. B. Dev, R. N. Mohapatra and Yongchao Zhang, JHEP **1605**, 174 (2016) [[arXiv:1602.05947](#) [hep-ph]].
- [8] A. Maiezza, M. Nemevsek and F. Nesti, Phys. Rev. Lett. **115**, 081802 (2015) [[arXiv:1503.06834](#) [hep-ph]]; M. Nemevsek, F. Nesti and J. C. Vasquez, [arXiv:1612.06840](#) [hep-ph].
- [9] G. Aad *et al.* [ATLAS Collaboration], JHEP **1503**, 041 (2015) [[arXiv:1412.0237](#) [hep-ex]]; CMS Collaboration, CMS-PAS-HIG-14-039; ATLAS Collaboration, ATLAS-CONF-2016-051.
- [10] D. Chang, R. N. Mohapatra and M. K. Parida, Phys. Rev. Lett. **52**, 1072 (1984).
- [11] G. Beall, M. Bander and A. Soni, Phys. Rev. Lett. **48**, 848 (1982); G. Ecker, W. Grimus and H. Neufeld, Phys. Lett. **127B**, 365 (1983); H. An, X. Ji, R. N. Mohapatra, and Yue Zhang, Nucl. Phys. B **802**, 247 (2008) [[arXiv:0712.4218](#) [hep-ph]]; A. Maiezza, M. Nemevsek, F. Nesti and G. Senjanovic, Phys. Rev. D **82**, 055022 (2010) [[arXiv:1005.5160](#) [hep-ph]]; M. Blanke, A. J. Buras, K. Gemmler and T. Heidsieck, JHEP **1203**, 024 (2012) [[arXiv:1111.5014](#) [hep-ph]]; S. Bertolini, A. Maiezza and F. Nesti, Phys. Rev. D **89**, 095028 (2014) [[arXiv:1403.7112](#) [hep-ph]].
- [12] S. R. Coleman and E. J. Weinberg, Phys. Rev. D **7**, 1888 (1973).
- [13] A. D. Linde, JETP Lett. **23**, 64 (1976); S. Weinberg, Phys. Rev. Lett. **36**, 294 (1976).
- [14] M. Holthausen, M. Lindner and M. A. Schmidt, Phys. Rev. D **82**, 055002 (2010) [[arXiv:0911.0710](#) [hep-ph]].
- [15] R. N. Mohapatra, Phys. Rev. D **34**, 909 (1986).
- [16] G. Senjanović and V. Tello, Phys. Rev. Lett. **114**, 071801 (2015) [[arXiv:1408.3835](#) [hep-ph]].
- [17] P. A. R. Ade *et al.* [Planck Collaboration], Astron. Astrophys. **594**, A13 (2016) [[arXiv:1502.01589](#) [astro-ph.CO]].
- [18] R. Babich, N. Garron, C. Hoelbling, J. Howard, L. Lellouch and C. Rebbi, Phys. Rev. D **74**, 073009 (2006) [[hep-lat/0605016](#)].
- [19] A. J. Buras, S. Jager and J. Urban, Nucl. Phys. B **605**, 600 (2001) [[hep-ph/0102316](#)].
- [20] C. Patrignani *et al.* (Particle Data Group), Chin. Phys. C, **40**, 100001 (2016).
- [21] P. S. B. Dev, R. N. Mohapatra and Y. Zhang, [arXiv:1703.02471](#) [hep-ph].
- [22] D. Becirevic, V. Gimenez, G. Martinelli, M. Papinutto and J. Reyes, JHEP **0204** (2002) 025 [[hep-lat/0110091](#)].
- [23] J. R. Batley *et al.* [NA48/2 Collaboration], Phys. Lett. B **677**, 246 (2009) [[arXiv:0903.3130](#) [hep-ex]].
- [24] J. R. Batley *et al.* [NA48/2 Collaboration], Phys. Lett. B **697**, 107 (2011) [[arXiv:1011.4817](#) [hep-ex]].
- [25] C. Lazzeroni *et al.* [NA62 Collaboration], Phys. Lett. B **732**, 65 (2014) [[arXiv:1402.4334](#) [hep-ex]].
- [26] A. Alavi-Harati *et al.* [KTeV Collaboration], Phys. Rev. Lett. **93**, 021805 (2004) [[hep-ex/0309072](#)].
- [27] A. Alavi-Harati *et al.* [KTEV Collaboration], Phys. Rev. Lett. **84**, 5279 (2000) [[hep-ex/0001006](#)].
- [28] E. Abouzaid *et al.* [KTeV Collaboration], Phys. Rev. D **77**, 112004 (2008) [[arXiv:0805.0031](#) [hep-ex]].
- [29] T. Alexopoulos *et al.* [KTeV Collaboration], Phys. Rev. D **70**, 092006 (2004) [[hep-ex/0406002](#)].
- [30] B. Aubert *et al.* [BaBar Collaboration], Phys. Rev. Lett. **91**, 221802 (2003) [[hep-ex/0308042](#)].
- [31] J.-T. Wei *et al.* [Belle Collaboration], Phys. Rev. Lett. **103**, 171801 (2009) [[arXiv:0904.0770](#) [hep-ex]].
- [32] R. Aaij *et al.* [LHCb Collaboration], JHEP **1302**, 105 (2013) [[arXiv:1209.4284](#) [hep-ex]].
- [33] V. V. Anisimovsky *et al.* [E949 Collaboration], Phys. Rev. Lett. **93**, 031801 (2004) [[hep-ex/0403036](#)].
- [34] A. V. Artamonov *et al.* [E949 Collaboration], Phys. Rev. Lett. **101**, 191802 (2008) [[arXiv:0808.2459](#) [hep-ex]].
- [35] A. V. Artamonov *et al.* [BNL-E949 Collaboration], Phys. Rev. D **79**, 092004 (2009) [[arXiv:0903.0030](#) [hep-ex]].
- [36] A. V. Artamonov *et al.* [E949 Collaboration], Phys. Rev. D **72**, 091102 (2005) [[hep-ex/0506028](#)].
- [37] J. P. Lees *et al.* [BaBar Collaboration], Phys. Rev. D **87**, no. 11, 112005 (2013) [[arXiv:1303.7465](#) [hep-ex]].
- [38] G. Anelli *et al.*, CERN-SPSC-2005-013, CERN-SPSC-P-326.
- [39] T. Abe *et al.* [Belle-II Collaboration], [arXiv:1011.0352](#) [physics.ins-det].
- [40] F. Bergsma *et al.* [CHARM Collaboration], Phys. Lett. **157B**, 458 (1985).
- [41] S. Alekhin *et al.*, Rept. Prog. Phys. **79**, no. 12, 124201 (2016) [[arXiv:1504.04855](#) [hep-ph]].
- [42] C. Adams *et al.* [LBNE Collaboration], [arXiv:1307.7335](#) [hep-

- ex].
- [43] G. Aad *et al.* [ATLAS Collaboration], [arXiv:0901.0512](#) [hep-ex].
- [44] G. L. Bayatian *et al.* [CMS Collaboration], *J. Phys. G* **34**, 995 (2007); S. Chatrchyan *et al.* [CMS Collaboration], *JINST* **3**, S08004 (2008).
- [45] B. Dasgupta, J. Kopp and P. Schwaller, *Eur. Phys. J. C* **76**, no. 5, 277 (2016) [[arXiv:1602.04692](#) [hep-ph]]; Y. Tsai, L. T. Wang and Y. Zhao, [arXiv:1603.00024](#) [hep-ph]; H. Fukuda, M. Ibe, O. Jinnouchi and M. Nojiri, [arXiv:1607.01936](#) [hep-ph].
- [46] J. P. Chou, D. Curtin and H. J. Lubatti, [arXiv:1606.06298](#) [hep-ph].